MONTANE FOREST WATER USE UNDER INCREASED EPISODIC AND EARLIER SNOWMELT

Ava Cooper[1] and Adrian Harpold[1]

EXTENDED ABSTRACT

Western U.S. montane forests rely disproportionately on snowmelt, which potentially makes them sensitive to changes in snowpack to alter large-scale water and carbon budgets. We used an aspect transect of sap flow and meteorological measurements in Sagehen Creek watershed, in the Sierra Nevada mountains, to empirically determine controls on the timing of water use by conifer forests. We determine which environmental variables (temperature, humidity, shortwave radiation, and soil moisture) are limiting sap flow across the growing season using a boundary lines analysis. We find that all sites exhibit transitions from energy limitations in spring, to water limitations in summer, and back to energy limitations in fall. Response of sap flow to predictors was more variable during spring than fall, which is consistent of more episodic temperature limitations in the spring. Later snowmelt leads to substantial transpiration prior to snow disappearance and trees were air temperature limited less of the time. Shifts from rain to snow under climate change might diminish existing forest refugia as snowmelt becomes more similar across slope aspects. Future efforts focused on modeling the relationship between snow water inputs and transpiration will be important to understanding the potential effects of climate change.

INTRODUCTION

Montane forests rely disproportionately on snowmelt in much of the Western U.S. (Hu et al., 2010; Trujillo et al., 2012). Spring snowmelt is starting and ending earlier and occurring at slower rates as a consequence of warmer temperatures in the Western U.S. (Harpold & Kohler, 2017; Harpold & Brooks, 2018; Mote et al., 2018; Musselman et al., 2017), but the response of forest's water use and carbon uptake is not well understood. Earlier snow water inputs and shifts from snow to rain will lead to earlier peak and seasonal recession of soil moisture (Harpold and Molotch, 2015). In areas with limited summer rain, earlier water inputs could increase late season soil water stress (Harpold, 2016), which increases the susceptibility of forests to disturbance (Hart et al., 2014). Forests' ability to shift the growing seasons earlier and withstand longer dry seasons is critical to developing mitigation strategies but remains challenging to observe and model. As a result, our understanding of snowpack dynamics influence on transpiration is insufficient for predicting the effects of climate change on larger-scale water and carbon budgets that provide critical natural resources.

Much of what is known about the impacts of snowmelt on forest productivity relies on studying cold, continental climates such as the Rocky Mountains, USA (Barnard et al., 2017; Bowling et al., 2018; Hu et al., 2010; Knowles et al., 2018; Winchell et al., 2016). Forests in the southern Rockies (Colorado and New Mexico) have continental climates with precipitation regimes that consist of winter snow and summer rain, often resulting in a bimodal shape in annual net ecosystem productivity (NEP) that is unique to the southern Rockies (Barnard et al., 2018). Research on tree water use in warmer, Mediterranean snowpacks, like the Sierra Nevada, USA, show the importance of intra- and inter-annual variability of water input dynamics (Kelly & Goulden, 2016; Goulden et al., 2012; Royce & Barbour 2001; Tague & Peng, 2013; Trujillo et al., 2012). Sierra Nevada forests typically exhibit more intermittent NEP at the start and end of the growing season than colder, continental sites caused by warm synoptic weather patterns, typical of the region, that can create temporary periods of water and energy availability during otherwise energy-limited periods (Barnard et al., 2018). Because snowmelt is the primary water input in Mediterranean climates, later water inputs from later snowmelt are correlated with higher productivity (Tague and Peng, 2013; Trujillo et al., 2012).

Paper presented Western Snow Conference 2019

[1] Ava Cooper, University of Nevada, Reno, Natural Resources and Environmental Sciences, Reno, NV, avac@nevada.unr.edu

[1] Adrian Harpold, University of Nevada, Reno, Natural Resources and Environmental Sciences, Reno, NV, aharpold@cabnr.unr.edu

Aspect and elevation act as broader controls on growing season length and spatial distribution of transpiration and south-facing sites typically have longer growing seasons and exhibit more cold-season transpiration response (Barnard et al., 2017). However, observations focused on inter-relationships between topography, snow, and forest water use nexus have largely been conducted in the Rocky Mountains due to a lack of observations in other hydroclimates in the Western U.S.

Forest water use in remote, snow covered areas is challenging to observe in space and time. The impacts of snowmelt on forest water use have been observed with both field (i.e. eddy covariance and tree sap flow) and remote (i.e. optical, hyperspectral, and thermal sensors) observations. Several studies have applied optical remote sensing to calculate the normalized difference vegetation index (NDVI) to relate forest greenness to snow cover properties (Trujillo et al., 2012). Remote sensing methods have the advantage of large spatial extents but have potentially low spatial and temporal resolution. Eddy covariance-based field observations are used to determining montane forest ET and NEP (Goulden et al., 2012; Hu et al., 2010; Kelly & Goulden, 2016; Winchell et al., 2016). Eddy covariance systems have a relatively large footprint, which is useful for estimating ecosystem-scale fluxes but does not resolve tree transpiration from understory transpiration or evaporation from water in vegetation canopy or soil evaporation. Sap flow systems measure the sap flux density (or sap flow) using a variety of heating-based sensors (Steppe et al., 2010). Sap flow allows transpiration to be observed at the tree scale in different slope aspects and elevations by placing multiple sensors in different topoclimate positions (Barnard et al., 2017). However, sap flux density is difficult to scale to transpiration due to assumption in sapwood area (Looker et al., 2016). Despite scaling limitations, sap flow sensors are capable of detecting seasonal transition in tree water use (Chan & Bowling, 2017) and can be combined with other environmental data (e.g. vapor pressure deficit, soil moisture, etc.) to better understand the controls of montane forest water use in topographically complex places (Barnard et al., 2017; Bowling et al., 2018; Looker et al., 2018).

Our objective is to develop sap flow observations in a montane, Mediterranean climate in order to better understand how earlier snowmelt, mediated by topography and climate variability, impacts forest water use. We focus on mechanisms controlling forest water use in spring using a hillslope-scale aspect gradient in the montane Conifer forests of the northern Sierra Nevada, USA. We use sap flow, meteorological, and hydrological measurements on north and south aspects to empirically determine controls on the timing and magnitude of transpiration. We address two questions using primarily empirical analyses of our field observations: 1) Under what conditions do trees use early season snowmelt water? 2) How does earlier and more episodic snowmelt predispose a site to late season water stress?

METHODS

Study Site

Sagehen Creek is a 28 km^2 snow-dominated watershed in the Eastern California Sierra Nevada (Figure 1a). It spans an elevation range of 1771 m - 2655 m and has a Mediterranean climate with wet, cold winters and dry, hot summers. Most of the precipitation in the watershed falls as snow and the majority of precipitation falls between November 1 and May 1. Sagehen has a mixed conifer forest of Jeffrey pine (*Pinus jeffreyi*) and Lodgepole pine (*P. contorta*) at lower elevations to White pine (*P. monticola*) and Red fir (*Abies magnifica*) at higher elevations.

Meteorological and Environmental Data

We collect air temperature (8 m and 30 m), relative humidity (8 m and 30 m) (HMP50-L Temperature/Relative Humidity; Vaisala Corporation, Helsinki, Finland), solar radiation (30 m) (LI200X Silicon Pyranometer; LI-COR, Inc., Lincoln, NE), wind speed (8 m and 30 m) (Wind Monitor 05103-L; R.M. Young Company, Traverse City, MI), barometric pressure (30 m) (PTB110 Barometer; Vaisala Corporation, Helsinki, Finland) , and snow water equivalent (SWE) (snow pillow) every 10 minutes at a 30 m meteorological tower (Tower 4). The tower has two co-located sap flow clusters on the north- and south-facing aspects (hereafter north site and south site) of the ridge that record data every 15 minutes (Figure 1b). The sap flow clusters measure sap flux density (TDP30; Dynamax, Inc., Houston, TX), surface temperature (SI-111; Apogee Instruments Inc., Logan, UT), soil moisture (10 cm, 30 cm, and 50 cm), soil temperature (10 cm, 30 cm, and 50 cm) (CS655; Campbell Scientific, Inc., Logan, UT), snow depth Figure 1c & 1d, Ultrasonic Depth Sensor; Judd Communications LLC, Salt Lake City, UT), and snow water equivalent (SWE plates; Trustman, 2016). All data were aggregated to hourly and daily averages. Daily averages were calculated as 10:00 to 15:00 for all variables and sap flux density to remove any influence of nighttime values from the analysis. Some short gaps (< 1 day) in data were filled with linear interpolation.

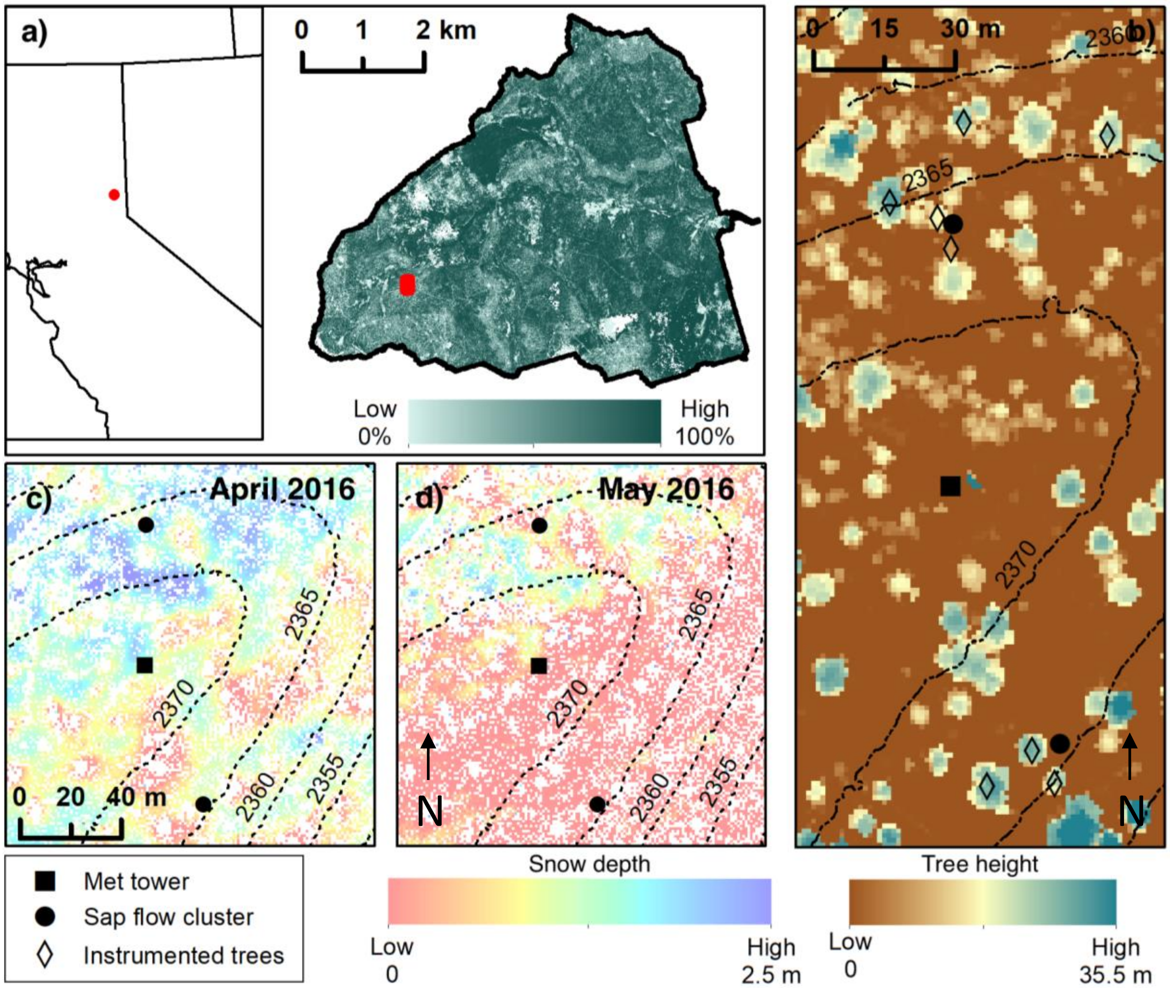

Figure 1. Site map of Sagehen Creek Watershed. a) Location of Sagehen Creek Watershed in California and watershed boundary showing forest cover in green (white is 0% forest cover) with location of site marked in red, b) Main tower and sap cluster locations with tree heights in meters and diamonds marking trees used in this study, c) April 2016 Airborne Snow Observatory (ASO) snow depth, and d) May 2016 ASO snow depth (missing data is shown as white).

Sap Flux Density Data and Processing

Sap flux density is a useful tree-level measurement to quantify vegetation water use. We use thermal dissipation probes (TDP30; Dynamax, Inc., Houston, TX) that return a millivolt difference (ΔT) between the two thermocouples. The millivolt difference between the probes is converted to a temperature difference. A zero-flow reference (hereafter baseline; ΔT_{max}) is required to calculate sap flux density from the recorded temperature differences (Equation 1).

A comprehensive study conducted by Peters et al. (2018) explored four different methods for determining baseline conditions. The daily predawn method forces every night to baseline conditions, however some evidence suggests that nighttime sap flow is possible given a high enough vapor pressure deficit (VPD) (Snyder et al., 2003). Differences in nighttime VPD may explain differences in the baselines and therefore the nighttime low sap flow values between Tower 4 and Tower 1. Other baseline correction methods allow for nighttime sap flow. We chose to use the double regression method as described by Lu et al. (2004) over the moving window (Rabbel et al., 2016) and environment dependent (Oishi et al., 2016) methods. The double regression methods accounts for nighttime flow and issues with a drifting baseline over the growing season. The moving window method (Rabbel et al., 2016) only accounts for nighttime flow and the environment dependent method (Oishi et al., 2016) requires is dependent on temperature and VPD conditions which may bias our later analyses that compare temperature, absolute humidity, and sap flux density.

In the double regression method, ΔT_{max} is calculated over 10-day periods and a linear regression is calculated through those values for the entire growing season. If a ΔT_{max} value is below the calculated regression line, it is removed, and the linear regression is re-calculated with the remaining points (Lu et al., 2004). We follow the standard Granier (1985) empirical equation for determining sap flux density (F_d) ($cm^3\ cm^{-2}\ h^{-1}$) (Equation 1) and use the calculated baseline from the double regression for the ΔT_{max} value:

$$F_d = 0.0119 * \left(\frac{\Delta T_{max} - \Delta T}{\Delta T}\right)^{1.231} \quad (1)$$

We filter the data for low voltage (< 2.9V) because lower voltages can cause spikes in the data. We also filter for data that do not follow a diurnal pattern (maximum during the day and minimum at night), which is indicative of transpiration. We used daily averages of the sap flux density data to calculate the fraction of total sap flow that occurred prior to snow disappearance for each site and year.

Principal Component Analysis and Interaction Variables

Environmental variables (air temperature, relative humidity, incoming shortwave radiation, and soil moisture) inherently co-vary diurnally and annually. Principal component analysis (PCA) is a useful tool for finding which variables co-vary by combining variables into uncorrelated principal components that are optimized for explaining variance in the target variable. Daily average data were normalized to remove relative scaling dependencies in the PCA. The analysis was limited to environmental variables, as we did not measure physiological variables such as leaf water potential. Sap flux density was the target variable for the PCA and the environmental variables were the predictors. We focused on the first two principal components as those explained approximately 90% of variance in sap flux density at each site. We used PCA to determine which variables have high interaction (loaded equally on the same components; Table S1). Potentially interactive variables were multiplied together and used in the boundary line analysis (e.g. [air temperature]*[incoming shortwave radiation]).

Boundary Line Analysis

Boundary line analysis is a common method for determining environmental and physiological limitations on stomatal conductance by finding the upper envelope of the relationship between explanatory variables and stomatal conductance (Chambers et al., 1985). We implemented boundary line analysis on daily average sap flux density as a function of the daily averages of different environmental variables and interaction variables. In our analysis, boundary lines represent maximum potential sap flux density under a certain environmental variable given optimal conditions of other environmental variables. We combined the north and south sites for the boundary line analysis because we use the same meteorological data for both sites and the only difference in inputs to the boundary line analysis is soil moisture. Daily average sap flux density data as a function of daily average environmental variables were grouped into bins of 50 counts along the x-axis (environmental variable). For each bin, the 95th percentile value was calculated to quantify the upper envelope. A potential sap flux density value was calculated for each day using linear interpolation across all observed values of the environmental variable based on the 95th percentile values from each bin. We excluded soil moisture and [soil moisture*shortwave] boundary line values above 2 cm of water content because they reflected only energy-limited periods. We compared daily potential sap flux densities between the different variables and selected the variable with the lowest potential sap flux density as the most limiting factor for that day.

Growing Season End

Potential sap flux densities use the same boundary line method but exclude soil moisture and [soil moisture*shortwave] to estimate sap flux density in non-water (soil moisture) limited conditions. We use a ratio of 0.5 between actual (i.e. measured) and potential (i.e. non-water limited) sap flux density as a metric for the end of the growing season. We compare the end of growing season calculated based on actual and potential sap flux density with the day of snow disappearance.

RESULTS AND DISCUSSION

Sagehen often lies within the rain-snow transition and experiences high interannual variability in the amount of snow it receives during the winter months. This study was conducted across 3 years: 2016 (average year; 135.4 cm precipitation), 2017 (wet year; 230.6 cm precipitation), and 2018 (drier than average year; 107.7 cm precipitation). Partitioning of precipitation to snow at peak snow accumulation (SWE/P) was quite different between the north- and south-facing aspects and slightly different between years (Figure 2a). The north and south sites had large differences in peak snow water equivalent (SWE), especially in 2017 (66 cm difference in SWE), the wettest year of the study (Figure 3d). Day of snow disappearance occurred latest in 2017 for both sites and earliest in 2018 for both sites (Figure 3d). The difference in timing of snow disappearance between sites was similar in all years with an average of 15 days earlier snow disappearance at the south site. Differences in SWE/P between the aspects were reflected in soil moisture differences between the two sites. Every year, the south site had more midwinter snowmelt pulses in the soil moisture, whereas the north site had more distinct diurnal snowmelt pulses at the end of spring snowmelt (Figure 3e). As a result, peak soil moisture at the north site was higher than the south aspect site in all years. The south site hit wilting point of shallow soil moisture (0.1 volumetric water content (VWC)) earlier and snow disappeared earlier than the north site in all years (Figure 2c). However, soil moisture at both sites decreased to similar minimum values in summer near 1.0 cm of water or 0.10 VWC (Figure 3e).

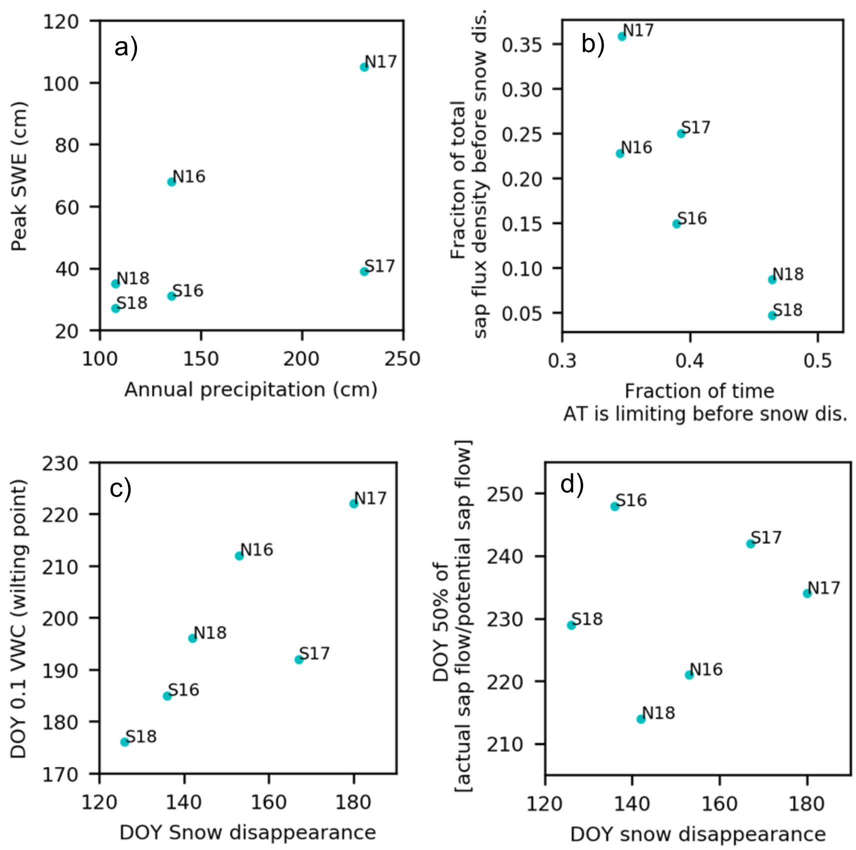

Figure 2. (a) Peak snow water equivalent as a function of annual precipitation for each aspect (S = south, N = north) and for all years. (b) Fraction of total sap flow that occurred prior to snow disappearance as a function of the fraction of time that air temperature was limiting prior to snow disappearance for all sites and years. (c) Day of year shallow soil moisture reached wilting point (0.1 VWC) as a function of snow disappearance for all sites and years. (d) End of growing season represented by say of year when the ratio of actual to potential sap reached 0.5 as a function of day of year of snow disappearance for all sites and years.

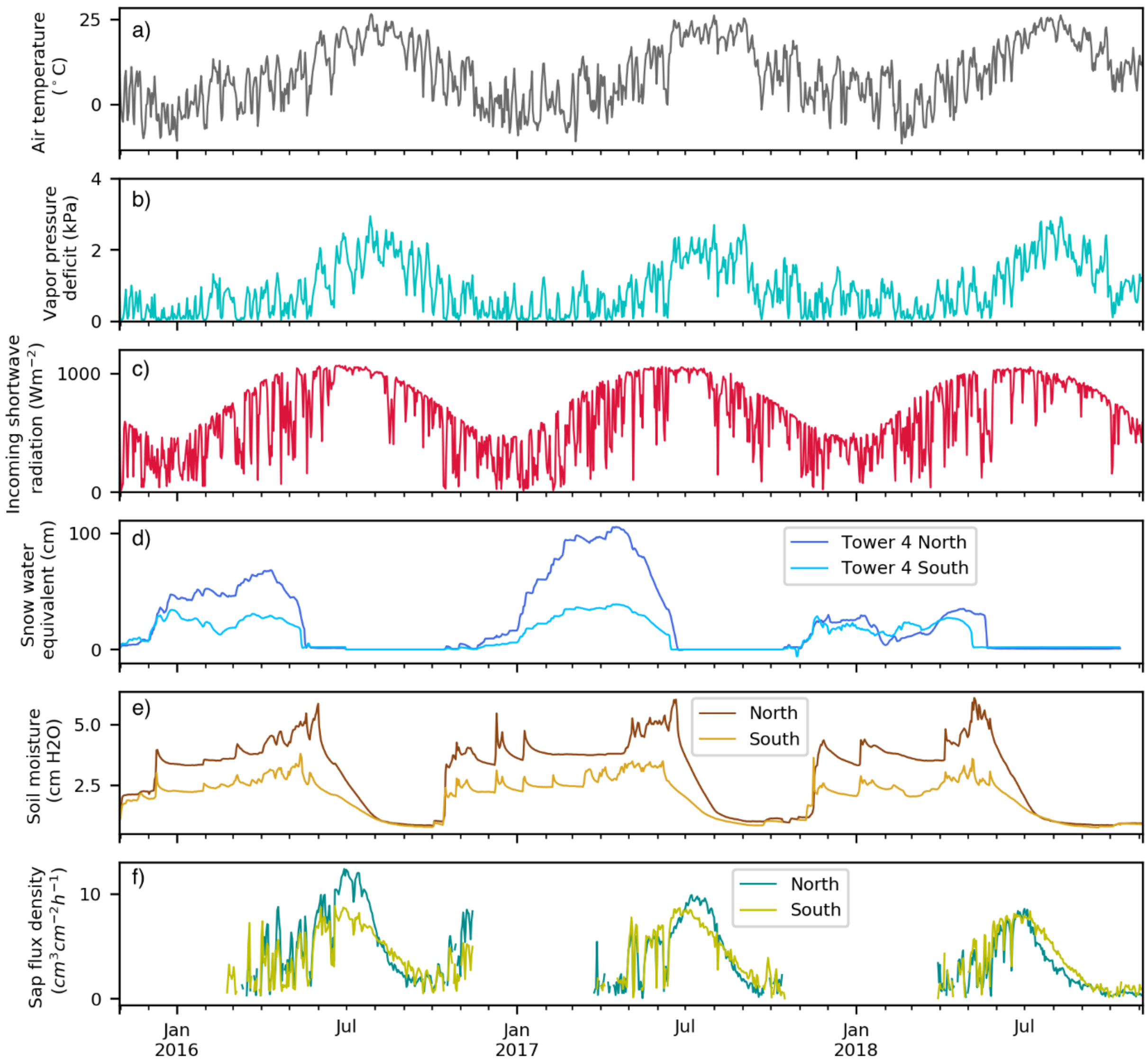

Figure 3. Daily (10:00 – 15:00) average data from the main 30 m meteorological tower and sap flow clusters (north and south). From the main tower: (a) air temperature (7.6 m), (b) vapor pressure deficit (VPD) (7.6 m), (c) incoming shortwave radiation. From the sap flow clusters: (7.6 m) snow water equivalent, (e) soil moisture content, (f) site average sap flux density.

Early-season sap flow (i.e. prior peak annual sap flow) was highly variable in all years and similar between north and south aspects. In 2016 and 2017, early-season sap flow diverged between the two aspects prior to peak sap flow and converged back to similar late season values after shallow soil moisture reaches wilting point at the north aspect site (Figure 4a and 4d). Sap flow was more similar between sites early and mid-growing season in 2018 but was higher at the south-facing site in July and August (Figure 4g). September and October rainfall sometimes supplemented soil moisture and caused a late season resurgence in sap flow, as seen in October 2016 (Figure 4a). The addition of late season soil moisture resulted in a return to energy-limitations (Figure 4b and 4c).

Boundary line analysis (BLA) shifts from sporadic energy-limited sap flow in the early season to consistent soil moisture limitation during the late season (Figure 4). Both north and south-facing sites have the same early season limitations because the same meteorological data are used for each site and soil moisture was the only different input into the BLA. Of the energy-limitations, air temperature was the dominant limiting factor prior to snow disappearance (between 44.6% and 63.8% of the time). Years and sites with higher SWE had higher ablation air temperatures and were temperature-limited less often than years and sites with lower peak SWE. The fraction of sap flow that occurred prior to snow disappearance was most different between sites in the wettest year (2017) and most similar in the driest year (2018) (Figure 2b). Both the sporadic behavior and the high fraction of time the sites were temperature-limited are similar to the synoptic weather-driven net ecosystem productivity (NEP) found in the southern Sierra Nevada (Kelly & Goulden, 2016). As seen in the southern Rockies, the energy required to melt a larger snowpack aligns with a warmer part of the seasonal temperature cycle and trees can use water more concurrently with snowmelt (Winchell et al., 2016).

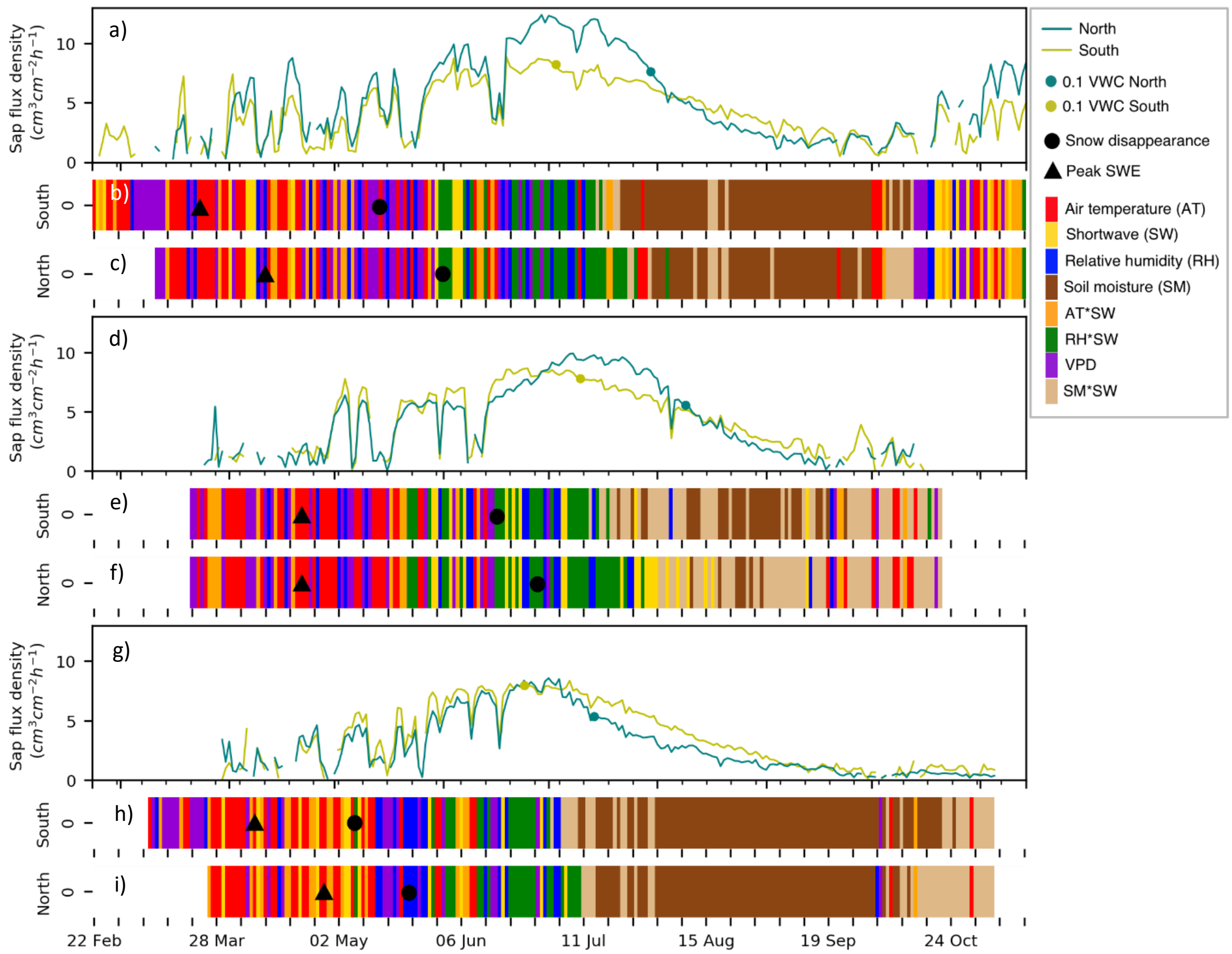

Figure 4. Daily average sap flux density and day of wilting point (0.1 volumetric water content) (colored circles) (a, d, g). Limiting factors from boundary line analysis, day of peak SWE (triangles), and day of snow disappearance (circles) for the south (b, e, h) and north (c, f, i) clusters for 2016 (a, b, c), 2017 (d, e, f), and 2018 (g, h, i).

Mid-to-late growing season, the south aspect reached soil moisture limitations prior to the north aspect in all years. In 2017, both sites experienced more soil moisture-shortwave limitations instead of predominantly soil moisture limitations as seen in the drier late seasons of 2016 and 2018. This might be a result of the entire growing season being shifted later in the year. Both sites reached shallow soil moisture wilting point (0.1 VWC) earlier in years with earlier snow disappearance ($r^2 = 0.65$) (Figure 2c). The south site reached wilting point earlier than the north site for the same day of snow disappearance. The relationship between snow disappearance and soil water stress was not reflected in the relationship between snow disappearance and metrics for the end of the growing season, highlighting the complexity of how water is partitioned in the system and the potential role of deeper water sources. The sap-flow-based growing season end metric had no clear relationship with snow disappearance (r^2 =

0.022, p-value = 0.78) (Figure 2d). However, it is important to note the more well-defined relationship between the north site and snow disappearance than the south site using the sap flow-based growing season method. The north site had a more defined pulse of snowmelt water at the end of spring snow ablation in all years which might have allowed that water to be more readily partitioned to transpiration whereas midwinter melt pulses at the south site could not be advantageously used by the trees due to energy limitations midwinter. Boundary line analysis and sap flow-based metrics for growing season timing presented in this work will be useful for future forest water use studies in snow-dominated montane forests.

CONCLUSIONS

Our analysis of forest water use across aspects of Sagehen Creek Watershed provides novel insight on mechanisms controlling tree-level water use during snowmelt and at the end of the growing season. Temperature limitations controlled sap flow during snowmelt and in years with earlier snowmelt, snowmelt occurred earlier in the seasonal temperature cycle, and sap flow was more often temperature-limited. The end of the growing season was consistently modulated by timing of water input and subsequent differences in the timing of soil moisture drying down in summer. However, it was difficult to gage late season forest water stress based on timing of snow disappearance, likely attributed to the complexity of snow-soil-vegetation interactions and deeper water storage that was not accounted for.

The Sierra Nevada experiences high interannual variability in precipitation, specifically variability in the rain-snow elevation line and whether precipitation is partitioned to snow. Differences in interannual precipitation combine with complex topographic controls on snow resulted in very different timing in soil water stress and forest water use between aspects at similar elevations. Snowmelt can be an opportunity for high productivity when it occurs later in the warmer part the seasonal temperature cycle. However, shifts from snow to rain are expected with climate change and this will have implications for the timing of water input and whether that water is partitioned to transpiration. Our work highlights a need for improved observation networks of forest water use to support improved empirical methods for determining growing season metrics and for validating transpiration values predicted by land surface models. (KEYWORDS: spring snowmelt, initiation of transpiration, sap flow, slope aspect, boundary line analysis)

REFERENCES

Barnard, D. M., Barnard, H. R., & Molotch, N.P. 2017. Topoclimate effects on growing season length and montane conifer growth in complex terrain. *Environmental Research Letters*, **12**, 64003.

Barnard, D. M., Hu, J., Goulden, M. L., Litvak, M. E., Barnard, H. R., Knowles, J. F., & Molotch, N. P. 2018. Reevaluating growing season length controls on net ecosystem production in evergreen conifer forests. *Scientific Reports*, **8**, 1–10.

Bowling, D. R., et al. 2018. Limitations to winter and spring photosynthesis of a Rocky Mountain subalpine forest. *Agricultural and Forest Meteorology*, **252**, 241–255.

Chambers, J. L., Hinckley, T. M., Cox, G. S., Metcalf, C. L., & Aslin, R. G. 1985. Boundary-line analysis and models of leaf conductance for four oak-hickory forest species. *Forest Science*, **31**, 437–450.

Chan, A. M., & Bowling, D. R. 2017. Assessing the thermal dissipation sap flux density method for monitoring cold season water transport in seasonally snow-covered forests. *Tree Physiology*, **37**, 984–995.

Goulden, M. L., Anderson, R. G., Bales, R. C., Kelly, A. E., Meadows, M., & Winston, G. C. 2012. Evapotranspiration along an elevation gradient in California's Sierra Nevada. *Journal of Geophysical Research: Biogeosciences*, **117**, 1–13.

Granier A. 1985. Une nouvelle methode pour la measure du flux de seve brute dans le tronc des arbres. *Annales des Sciences Forestieres* **42**, 193–200.

Harpold, A. A. 2016. Diverging sensitivity of soil water stress to changing snowmelt timing in the Western U.S. *Advances in Water Resources*, **92**, 116–129.

Harpold, A. A., & Brooks, P. D. 2018. Humidity determines snowpack ablation under a warming climate. *Proceedings of the National Academy of Sciences*, **115**, 1215 – 1220.

Harpold, A. A., & Kohler, M. 2017. Potential for Changing Extreme Snowmelt and Rainfall Events in the Mountains of the Western United States. *Journal of Geophysical Research: Atmospheres*, **122**, 13,219-13,228.

Harpold, A. A., & Molotch, N. P. 2015. Sensitivity of soil water availability to changing snowmelt timing in the western U.S. *Geophysical Research Letters*, **42**, 8011–8020.

Hart, S. J., Veblen, T. T., Eisenhart, K. S., Jarvis, D., & Kulakowski, D. 2014. Drought induces spruce beetle (Dendroctonus rufipennis) outbreaks across northwestern Colorado. *Ecology*, **95**, 930 - 939.

Hu, J., Moore, D. J. P., Burns, S. P., & Monson, R. 2010. Longer growing seasons lead to less carbon sequestration by a subalpine forest. *Global Change Biology*, **16**, 771–783.

Kelly, A. E., & Goulden, M. L. 2016. A montane Mediterranean climate supports year-round photosynthesis and high forest biomass. *Tree physiology*, **36**, 459–468.

Knowles, J. F., Molotch, N. P., Trujillo, E., & Litvak, M. E. 2018. Snowmelt-driven tradeoffs between early and late season productivity negatively impact forest carbon uptake during drought. *Geophysical Research Letters*, **45**, 3087 – 3096.

Looker N, Martin J, Hoylman Z, Jencso K, Hu J. 2018. Diurnal and seasonal coupling of conifer sap flow and vapour pressure deficit across topoclimatic gradients in a subalpine catchment. *Ecohydrology*. 2018;e1994.

Looker, N., Martin, J., Jencso, K., & Hu, J. 2016. Contribution of sapwood traits to uncertainty in conifer sap flow as estimated with the heat-ratio method. *Agricultural and Forest Meteorology*, **223**, 60–71.

Lu, P., Urban, L., & Zhao, P. 2004. Granier's thermal dissipation probe (TDP) method for measuring sap flow in trees: Theory and practice. *Acta Bontanica Sinica*, **46**, 631 - 646.

Mote, P. W., Hamlet, A. F., Clark, M. P., & Lettenmaier, D. P. 2005. Declining mountain snowpack in western north America. Bulletin of the American Meteorological Society, 86(1), 39–49.

Musselman, K. N., Clark, M. P., Liu, C., Ikeda, K., & Rasmussen, R. 2017. Slower snowmelt in a warmer world. *Nature Climate Change*, **7**, 214–219.

Oishi, A. C., Hawthorne, D. A., & Oren, R. 2016. Baseliner: An open-source, interactive tool for processing sap flux data from thermal dissipation probes. *SoftwareX*, **5**, 139–143.

Peters, R. L., et al. 2018. Quantification of uncertainties in conifer sap flow measured with the thermal dissipation method. *New Phytologist*, **219**, 1283–1299.

Rabbel, I., Diekkrüger, B., Voigt, H., & Neuwirth, B. 2016. Comparing ΔTmax Determination Approaches for Granier-Based Sapflow Estimations. *Sensors*, **16**, 2024.

Snyder, K. A., Richards, J. H., & Donovan, L. A. 2003. Night-time conductance in C3 and C4 species: do plants lose water at night? *Journal of Experimental Botany*, **54**, 861–865.

Steppe, K., De Pauw, D. J. W., Doody, T. M., & Teskey, R. O. 2010. A comparison of sap flux density using thermal dissipation, heat pulse velocity and heat field deformation methods. *Agricultural and Forest Meteorology,* **150**, 1046–1056.

Swetnam, T. L., Brooks, P. D., Barnard, H. R., Harpold, A. A., & Gallo, E. L. 2017. Topographically driven differences in energy and water constrain climatic control on forest carbon sequestration. *Ecosphere*, **8**.

Tague, C., & Peng, H. 2013. The sensitivity of forest water use to the timing of precipitation and snowmelt recharge in the California Sierra: Implications for a warming climate. *Journal of Geophysical Research: Biogeosciences*, **118**, 875–887.

Trujillo, E., Molotch, N. P., Goulden, M. L., Kelly, A. E., & Bales, R. C. 2012. Elevation-dependent influence of snow accumulation on forest greening. *Nature Geoscience*, **5**, 705–709.

Trustman, B. 2016. Characterizing Spatial and Temporal Variability of Snow Water Equivalent Using Pressure Sensors (master's thesis). Retrieved from Proquest. (Accession No. 10126128).

Winchell, T. S., Barnard, D. M., Monson, R. K., Burns, S. P., & Molotch, N. P. 2016. Earlier snowmelt reduces atmospheric carbon uptake in midlatitude subalpine forests. *Geophysical Research Letters*, **43**, 8160–8168.